The Response of a Radio-Astronomy Synthesis Array to Interfering Signals

A. RICHARD THOMPSON, SENIOR MEMBER, IEEE

Abstract—**Multiplying interferometers, and the more complex synthesis arrays that have been developed from them, possess the advantage of greater discrimination against interfering signals than can be obtained with single-antenna radio telescopes. The major contribution to this effect results from the relative changes of the phases of the signals received in spaced antennas, associated with the sidereal motion of a cosmic source across the sky. Signals that do not show this predictable phase behavior are substantially suppressed in the data processing. In this paper an approximate general expression for the interference response is derived and compared with results of an experimental test. The major uncertainty results from the variability of the gain of the antenna sidelobes in which the interference is received. Threshold levels at which interference becomes harmful are derived for the very large array (VLA) of the National Radio Astronomy Observatory. In the case of broad-band interfering signals, further rejection occurs because inequalities in the time delays of the signal paths via the individual antennas result in decorrelation. The magnitude of the decorrelation depends upon the position of the source of interference, and as an example, computations are given for broad-band signals from a satellite in geostationary orbit. General thresholds for harmful interference to radio astronomy are given in International Radio Consultive Committee (CCIR) Report 224, and the present results are not intended to supercede them. Rather, the intention is to provide data specific to synthesis arrays to allow more accurate coordination in certain frequency ranges shared with active spectrum users. A possible application to the search for extraterrestrial intelligence is mentioned.**

I. INTRODUCTION

BECAUSE OF their high sensitivity, radio telescopes are vulnerable to interference from other spectrum users. Telescopes that measure the total incident power in a single antenna are usually the most vulnerable, whereas interferometers that measure the correlation of signals received in two spaced antennas respond less strongly to interference. This desirable property of interferometers was first pointed out about 30 years ago by Ryle [1]. Modern instruments of this type which incorporate more than two antennas are often referred to as synthesis arrays.

Threshold levels of interference harmful to radio astronomy are specified in Report 224-4 of the International Radio Consultative Committee (CCIR) [2]. These levels are based upon the use of single-antenna telescopes, and interference received in sidelobes of gain 0 dBi.[1] In this paper interference levels for synthesis arrays are examined. The behavior of such an array is quite complicated, and depends upon parameters of the instrument, data processing techniques, and the position of the object being observed. The fact that, as will presently appear, the thresholds for synthesis arrays are higher than those in CCIR Report 224-4 must not be taken to imply that higher levels of interference are now acceptable within the frequency bands allocated to radio astronomy. Synthesis arrays are not applicable to all types of radio astronomy investigations. However, radio astronomers are often obliged to observe outside of the bands in which their service has a primary and exclusive frequency allocation, for example in studies of some radio lines. Coordination with other services is then necessary, and this often involves considerations specific to a particular observatory. Estimates of interference thresholds for different types of telescopes are therefore essential. Coordination is becoming increasingly important with the growing use of satellites, particularly those in geostationary orbit, and the practice of placing communications repeaters on the peaks of mountain ranges which have heretofore provided shielding to radio observatories. Preliminary results of the present study have been quoted with reference to a satellite power system [3], [4].

Manuscript received January 27, 1981; revised August 17, 1981. The National Radio Astronomy Observatory is operated by Associated Universities, Inc., under contract with the National Science Foundation.

The author is with the Very Large Array Program, National Radio Astronomy Observatory, Socorro, NM 87801.

[1] dBi indicates decibles relative to an isotropic radiator.

II. PRINCIPLES OF FOURIER SYNTHESIS MAPPING

Consider two antennas both pointed toward the same area of the sky, and let the outputs of the signal amplifiers expressed as complex functions of time be $e_1(t)$ from one antenna and $e_2(t)$ from the other. The antennas are connected to a receiving system that forms the time average of the product $e_1(t)e_2^*(t)$, using a multiplier that incorporates a signal-averaging circuit. When appropriately calibrated, this quantity is known as the complex visibility V. The inputs to the multiplier consist of components resulting from the wanted signal, the interference, and the system noise, which will be designated by subscripts s, i, and n, respectively. Thus:

$$V = \overline{(e_{1s} + e_{1i} + e_{1n})(e_{2s}^* + e_{2i}^* + e_{2n}^*)}$$

$$= V_s + V_i + V_n + \overline{\text{cross products}} \quad (1)$$

where the bar denotes an average. Here, V_s, V_i, and V_n are the components of V that would be measured if only the signal, the interference, or the noise were nonzero. The cross products represent noise. They are small compared with V_n, and can be neglected, provided that V_s and V_i are small compared with V_n. This condition is met in the consideration of harmful interference thresholds which follows.

The wanted component V_s is a function of the brightness pattern under observation and the vector spacing of the antennas. It is usual to specify the spacing in terms of u and v, the components projected onto a plane normal to the direction of the center of the area of sky under observation, u being measured toward the east and v toward the north as in Fig. 1. The units of u and v are wavelengths at the center frequency of the receiving passband. It can be shown [5], that with certain assumptions, the two-dimensional function $V_s(u, v)$ is the Fourier transform of $B_s(x, y)$ the desired brightness distribution on the sky. The procedure is therefore to measure the visi-

0018-926X/82/0500-0450$00.75

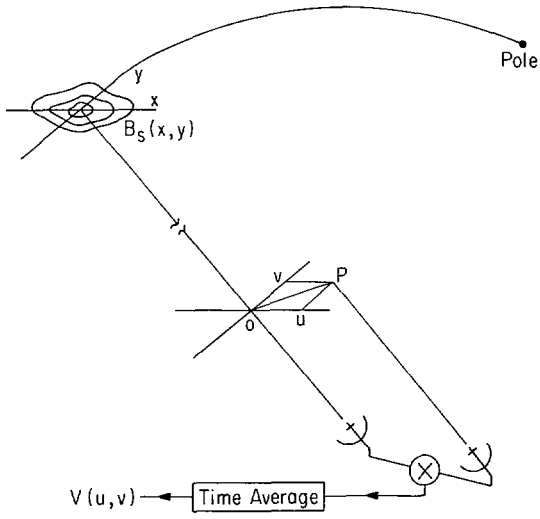

Fig. 1. Principle of Fourier synthesis mapping. $B_s(x, y)$ represents radio brightness of a source under observation, the y-axis being in the north direction as defined by a great circle through the pole. The antennas track the source position, which is the origin of the (x, y) coordinates. The antenna spacing projected onto a plane normal the direction of the source position is represented by the vector OP, which has components u and v measured in wavelengths toward the east and north, respectively. Fourier transformation of the visibility function, $V(u, v)$ yields a representation of $B(x, y)$.

bility over a sufficient range of points in the (u, v) plane and apply an inverse Fourier transform to obtain a map of the sky. Since the three components of the visibility cannot be separated, the transformation is applied to their sum V and the map obtained $B(x, y)$, is the sum of B_s and unwanted components B_i and B_n. Notice that corresponding components such as V_i and B_i are also Fourier pairs.

Two methods can be used to vary u and v: tracking the point of interest across the sky or moving one of the antennas to different locations. The components u and v are given by

$$u = L_x \sin H + L_y \cos H$$

$$v = L_z \cos \delta - L_x \sin \delta \cos H + L_y \sin \delta \sin H \qquad (2)$$

where H and δ are the hour angle and declination of the source position and L_x, L_y, and L_z are components of the baseline between the two antennas measured in wavelengths in the directions $(H = 0^\circ, \delta = 0^\circ)$, $(H = -90^\circ, \delta = 0^\circ)$ and $(\delta = +90^\circ)$, respectively. As H varies linearly with time, the spacing vector in the (u, v) plane traces out an arc of an ellipse. This locus may be almost circular for a source near the pole, or highly elongated for a source near the celestial equator. Since B_s is real, $V_s(u, v) = V_s^*(-u, -v)$, so any one measurement provides data at two conjugate points in the (u, v) plane. To obtain sufficient coverage if only two antennas are used, it is necessary to move one of them a number of times, tracking the source across the sky in each new configuration. If a larger number of antennas m is available, $m(m-1)/2$ signal products can be formed simultaneously, and it may be possible to map a source in a single passage. For further descriptions of synthesis mapping see [5], [6].

III. THE VERY LARGE ARRAY

The very large array (VLA) [7], used here as an example of a synthesis array, is located in New Mexico, and consists of 27 antennas arrayed on the three arms of an equiangular Y-shaped configuration. The resulting 351 antenna-pair combinations allow a detailed map to be obtained in a single period of 8 h or less. The antennas are fully steerable reflectors of diameter 25 m, with feeds that provide separate outputs for opposite senses of circular or linear polarization. The receiving electronics is tuneable over the following bands: 1340–1730 MHz (18–21 cm wavelength), 4.5–5.0 GHz (6 cm wavelength), 14.4–15.4 GHz (2 cm wavelength), and 22–24 GHz (1.3 cm wavelength). The antennas can be moved between different foundations by means of a rail-mounted transporter to allow the scale of the antenna spacings to be varied in four steps. In these configurations the most distant antenna on each arm is 0.6, 2, 6, or 21 km from the array center.

IV. THE AVERAGING EFFECT

Two effects reduce the response of a synthesis array to interference. The first, which we now consider, applies to any interfering signal, whereas the second applies only to broadband signals and is discussed in Section VIII. In a synthesis array the antenna outputs are combined in a way that maximizes the response to a source that moves across the sky as the earth rotates. In contrast, an interfering transmitter will be considered to remain fixed relative to the earth. The motion of the source results in changes in the relative phases of the signals at the antennas, and if the signals from any pair of antennas are simply multiplied together they produce a voltage that varies quasi-sinusoidally[2] with time. The output frequency is termed the natural fringe frequency, and depends upon the spacing of the antennas and the position of the radio source in the sky. Typically it is between a few millihertz and a few tens of hertz. In the VLA, time-varying phase changes are introduced into the local oscillator system which reduce the frequency of the output of the signal multipliers to zero. The required phase changes are computed for a hypothetical point source at a phase-reference position, which is usually the center of the area of sky being mapped. Two multipliers are used for each antenna pair, one having a quadrature phase shift at one input, so that the two time-averaged products represent the real and imaginary parts of $V(u, v)$. Because of the introduced phase changes, a signal from a stationary source, for which the relative phase at two antennas remains constant, produces a component at the multipliers that varies at the natural fringe frequency.

The multiplier outputs are digitized, and in the subsequent processing, these data, which correspond to points on the elliptical loci in the (u, v) plane, are interpolated to provide visibility values at points on a rectangular grid with equal spacings Δu and Δv in the u and v coordinates, respectively. Fourier transformation can then be performed using the fast algorithm for discretely sampled data. The simplest and most frequently used interpolation method is cell averaging [8] in which the (u, v) plane is divided into square cells of size Δu by Δv centered on the interpolation points, and the mean of all visibility values that fall within each cell is assigned to the central point. Thus the final averaging applied to the data before Fourier transformation depends upon the time taken for the antenna spacing vector to cross the corresponding cell. If τ is the cell-crossing time, the averaging reduces the inter-

[2] The fringe frequency varies slowly with time so the waveform is not precisely sinusoidal.

ference by a factor

$$F_1 = \sin(\pi f\tau)/\pi f\tau. \tag{3}$$

Here f is the natural fringe frequency which is given by

$$f = \omega_0 u \cos\delta \tag{4}$$

where ω_0 is the angular rotation velocity of the earth. Note that the interference reduction becomes ineffective as F_1 approaches unity, i.e., for a source near the pole, or for any source when the spacing vector crosses the v axis.

The first step in evaluating the response to interference is to calculate the mean squared value of F_1 over the (u, v) loci. To do this we introduce the (u', v') plane where $u' = u$ and $v' = v \csc\delta$. In the (u', v') plane the elliptical loci of the (u, v) plane become circles of radius $q' = (L_x^2 + L_y^2)^{1/2}$. Each circular locus is centered on the v' axis and is generated by a radius vector that rotates with a constant angular velocity ω_0. The cells in the (u', v') plane are elongated in the v' direction. Consider the locus for an antenna pair crossing a cell at a point where the radius vector makes an angle ϕ with the v' axis. If ϕ is small the path length through a cell is closely equal to Δu, and $f\tau = \phi\Delta u \cos\delta$. Now in practice Δu is unlikely to be less than 60 wavelengths; Δu^{-1} is the width of the synthesized field which is limited by the beamwidth of the individual antennas. Commonly used values of Δu are 100 to a few thousand wavelengths. For $\Delta u = 100$ and $\delta < 70°$, F_1^2 goes from 1.0 to $<3 \times 10^{-3}$ as ϕ increases from 0 to 10°. Thus we may use a small-ϕ approximation in deriving $\overline{F_1^2}$:

$$\begin{aligned}\overline{F_1^2} &= \frac{2}{\pi}\int_0^{\pi/2} F_1^2\, d\phi \\ &\cong \frac{2}{\pi}\int_0^{\infty} \frac{\sin^2(\pi\phi\Delta u\cos\delta)}{(\pi\phi\Delta u\cos\delta)^2}\, d\phi \\ &= \frac{1}{\pi\Delta u\cos\delta}.\end{aligned} \tag{5}$$

Note that when the above approximation fails, it does so first at declinations near the pole where $\cos\delta$ is small.

Let F_i be the power flux density of an interfering signal, and G_s be the effective gain of the antenna sidelobes in which it is received. Then the amplitude of the interference component at the multiplier output is

$$gG_sF_i\lambda^2/4\pi \tag{6}$$

where g is a gain factor of the receiving system and λ is the wavelength. After averaging over the cells of the (u, v) plane, the sum of the squared modulus of the interference component at the grid points is

$$\sum_N |V_i|^2 = N\alpha(gG_sF_i\lambda^2/4\pi)^2\overline{F_1^2}. \tag{7}$$

Here N is the number of cells in the (u, v) plane intersected by one or more spacing-vector loci, and α is the fraction of the loci which cross the v axis, where the major contribution to $|V_i|^2$ occurs. If the duration of the observation is less than 12 h, α may be less than unity. Following the usual notation for the discrete Fourier transform, e.g., [9], and using Parseval's theorem we obtain

$$n^2\overline{B_i^2} = N\alpha(gG_sF_i\lambda^2/4\pi)^2\overline{F_1^2}/n^2 \tag{8}$$

where $n \times n$ are the dimensions of the $V(u, v)$ and $B(x, y)$ arrays.

Suppose that the area of sky being mapped contains only a point source of spectral power flux density[3] F_s. The modulus of the corresponding visibility component is

$$gG_mF_s\beta\lambda^2/8\pi \tag{9}$$

where G_m is the main beam gain, β is the receiving bandwidth, and a factor of ½ is included because the antennas can accept only half the power in the randomly polarized cosmic signal. Suppose also that the source is located at the phase reference position. The imaginary component of the visibility is then zero. The resulting data are identical in each sampled cell, and after Fourier transformation they produce a peak of amplitude $B_s(0, 0)$ at the origin of the (x, y) plane given by

$$B_s(0, 0) = NgG_mF_s\beta\lambda^2/8\pi n^2. \tag{10}$$

Equations (8) and (10) provide the ratio of $(B_i)_{\text{rms}}$ to $B_s(0, 0)$, and by putting $F_s = 1.0$, $(B_i)_{\text{rms}}$ is obtained in units equal to the response to a point source of unit spectral power flux density. Thus we obtain

$$(B_i)_{\text{rms}} = \frac{2F_iG_s\sqrt{\alpha}}{G_m\beta\sqrt{\pi N\Delta u\cos\delta}}. \tag{11}$$

It has been assumed that no more than one locus falls within any of the N sampled cells of the (u, v) plane, but if Δu is larger than the spacing between adjacent loci, there will be, on average, n_l loci within each such cell, where $n_l > 1$. The right side of (11) should then be multiplied by $n_l^{-1/2}$. Note that the product $Nn_l\Delta u$ is essentially independent of the choice of Δu, and hence so is $(B_i)_{\text{rms}}$.

After cell averaging the interference component varies in a largely random manner, since the natural fringe period and the cell-crossing times are unrelated. In the map domain the randomness can be expected to produce a noise-like appearance in the interference component, and the concentration of large values near the v axis should result in elongation of the structure in directions close to east-west. This applies, of course, only to a steady interfering signal; bursts of intermittent duration can cause quite different distributions in the (u, v) plane. The response to interference is sometimes described as similar to the response to a hypothetical cosmic source at the pole which, like the interfering transmitter, remains fixed relative to the array. In this analogy the array would be randomly phased and the east-west structure corresponds to distant sidelobes of the synthesized response to the polar source.

V. VARIATION OF SIDELOBE GAIN

The sidelobe gain is not, of course, a constant, and as the antennas track the received interference varies with time.

[3] F_s is spectral power flux density measured in units of $\text{Wm}^{-2}\,\text{Hz}^{-1}$, whereas F_i is power flux density measured in Wm^{-2}. This terminology is consistent with CCIR definitions [10]. One millijansky (mJy) = $10^{-29}\,\text{Wm}^{-2}\text{Hz}^{-1}$.

Large amplitudes in the averaged data are not precisely centered on the v axis, but show some scatter corresponding to the occurrance of high sidelobes. Also, the reduction of the interference may be less efficient by a small factor than the above calculation indicates.

Part of the variation of the received interference can be ascribed to variation of the polarization characteristics of the sidelobes, which, in general, are not matched to the interfering signal. On average, only half of the power is received. However, for the peak levels of the received interference, which make a large contribution to interference in the map, the mismatch loss cannot be large. A correction for polarization mismatch would thus involve a factor of approximately two, and would be of comparable magnitude and opposite sense to a correction for the averaging efficiency mentioned above. Both effects have been omitted from the derivation in Section IV.

For any antenna pair the squared modulus of the correlator output is proportional to the product of the antenna gains. Thus is is apparent that the factor G_s^2 in (7) represents the product of the sidelobe gains averaged over angle. To the extent that the sidelobe patterns of the antennas are identical, G_s is a root mean square (rms) average which enhances the effect of high gain peaks.

VI. AN EXPERIMENTAL INVESTIGATION

To investigate the effects described in Sections IV and V, a map of a radio source was made in the presence of a constant controlled interfering signal. The observation was made during the construction phase of the VLA, and 14 antennas were available.[4] The source, 0537 + 531,[5] was mapped using a center frequency of 1430 MHz and bandwidth of 12 MHz. The observation covered an hour angle range of −5.2 to 4.8 h, and for 5 min out of every 20 min a calibration source 0552 + 389 was observed. This is a usual procedure in synthesis mapping, the calibration observations being used to provide a measure of the instrumental gain and phase characteristics.

A transmitter radiating 1 mW at 1427 MHz through a horizontally polarized horn of gain 5 dB was set up on a nearby mountain. Relative to the center of the array, the position of the transmitter was azimuth 106°, elevation 1.6°, and range 41 km. The signal strength at the array site was -126 ± 3 dB Wm^{-2}, based on an average of measured and calculated values. The transmitter was turned off during the calibration observations.

Fig. 2 shows one quadrant of a map from the above measurements, in which the brightness is the mean of that derived for two sets of data with opposite senses of polarization. The rms level of the interference over the map is 2.9 mJy, and this value can be used with (11) to estimate G_s, which is the least well known of the parameters involved. The other parameters for the map are $G_m = 48.4$ dBi, $\beta = 12$ MHz, $\Delta u = 134$ wavelengths, $N = 1.48 \times 10^4$, $\delta = 53.2°$, and $\alpha = 0.5$. If it is assumed that the interference data for the two polarizations combine with random phases, the resulting value of G_s is -7.3 ± 3 dBi.

During the observation the angle between the main beam and the transmitter direction increased steadily from 66° to 138°. Spectrum-analyzer measurements of the level of the interfering signal received at one antenna were used to obtain an approximate indication of the sidelobe gain. For angles of 66° to 100° from the main beam the mean gain was about −10 dBi, with occasional peaks as high as −5 dBi, the widths of the peaks being comparable to the main beam. The highest levels occured near 108° at which angle the Cassegrain subreflector just becomes occulted by the edge of the main reflector. The gain fell to −15 dBi or less at an angle of 118° and remained below that level as the angle from the main beam increased further. An examination of the averaged data at the grid points in the (u, v) plane showed that 20 percent of spacing loci that went through $u = 0$ showed high amplitudes corresponding to sidelobe levels of −3 to −8 dBi. For the antennas involved the v-axis crossings occured when the angle between the transmitter and the main beam was less than 110°. Thus the response to the interference was dominated by a small number of antenna pairs for which the v-axis crossings happened to coincide with high sidelobe levels in the direction of the transmitter.

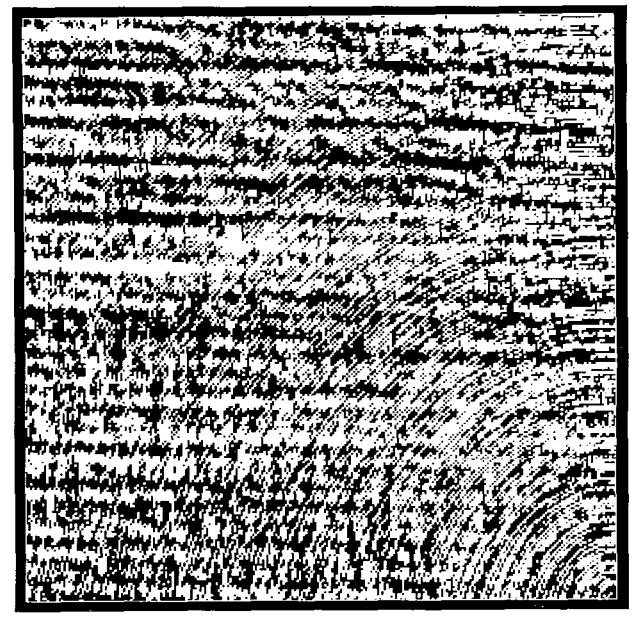

Fig. 2. One quadrant of a map of total dimensions 512 × 512 sample points, for which $\Delta u = 134$ wavelengths. The response to 0531 + 537 is in the bottom right-hand corner. Grating rings surrounding the source and the east-west structure in the interference are clearly visible.

VIII. DERIVATION OF HARMFUL LIMITS

From the results of Section IV it is possible to specify the rms level of the interference in a synthesized map in terms of the power flux density of the signal F_i. It is therefore possible to specify a level of F_i above which the interference becomes harmful to astronomical data. The usual criterion, e.g., [2], is that the harmful threshold occurs when the interference equals 1/10 of the rms noise level which sets the fundamental limit in the final data.

To compare the rms levels of the interference and noise note that the modulus of the rms system noise, after integration for a period τ, is

$$|V_n| = gkT_s\beta^{1/2}\tau^{-1/2} \tag{12}$$

[4] The date of the experiment was July 22, 1979 and the antennas used were at stations AW1, AW2, AW3, AW5, AN7, AW8, DN2, DN4, DN6, DE3, CE2, CE6, CE8, CE9; for an explanation of this nomenclature see [7].

[5] The nomenclature for radio sources follows that recommended in [11].

where k is Boltzmann's constant and T_s is the system noise temperature. The sum of the squared values of $|V_n|$ over the sampled (u, v) cells is

$$\sum_N |V_n|^2 = (gkT_s)^2 \beta \sum_N \tau^{-1}. \tag{13}$$

The mean value of τ^{-1} around a locus in the (u, v) plane is derived in the Appendix. Then from (5), (7), (13), (A2), and Parseval's theorem,

$$\frac{(B_i)_{\text{rms}}}{(B_n)_{\text{rms}}} = \frac{(|V_i|)_{\text{rms}}}{(|V_n|)_{\text{rms}}} = \frac{G_s F_i \lambda^2 \sqrt{\alpha}}{4\pi k T_s \sqrt{2\omega_0 \beta \cos\delta (1 + |\sin\delta|)}} \left[\frac{1}{N}\sum_N q'\right]^{-1/2}. \tag{14}$$

If the factor $\sqrt{\cos\delta\ (1 + |\sin\delta|)}$ is set to unity, the resulting error is less than 1 dB for $0 < \delta < 71°$, and 2.3 dB at $\delta = 80°$. For the interference threshold criterion, $(B_i)_{\text{rms}} = (B_n)_{\text{rms}}/10$,

$$F_i = \frac{0.4\pi k T_s \sqrt{2\omega_0 \beta}}{G_s \lambda^2 \sqrt{\alpha}} \left[\frac{1}{N}\sum_N q'\right]^{1/2}. \tag{15}$$

Table I contains numerical results for the VLA derived from (15), with parameter values as follows. As in [2], 0 dBi is used for the sidelobe gain. For the system noise temperature, 50 K is used for all bands: it is the current value for the 18–21 and 6 cm bands, and allows for planned improvements at 2 and 1.3 cm. The factor α is set to unity so that the results are applicable to long observation times. The intermediate frequency (IF) bandwidth in the VLA can be varied in steps of factors of two from 50 MHz down to 195 kHz. For observations of the continuum spectrum of radio sources the minimum bandwidth likely to be used is 6.25 MHz. For observations of spectral lines, in which a multichannel data-analysis technique is used, the narrowest channel bandwidth is 381 Hz [7]. In either case the narrowest bandwidth is used in Table I since this corresponds to the greatest sensitivity to interference. Finally, the mean value of q' over the sampled cells of the (u, v) plane is equal to the mean over 351 baselines weighted in proportion to the number of cells intersected by the corresponding locus, i.e.,

$$\frac{1}{N}\sum_N q' = \sum_{351} q'^2 \Big/ \sum_{351} q'. \tag{16}$$

Evaluation of (16) for the most compact configuration of the VLA, which is the one most sensitive to interference, yields 436 m divided by the appropriate wavelength, and this value is used in Table I. With the most extended configuration, the corresponding thresholds are 7.7 dB greater. For broad-band signals which cover the entire receiving bandwidth, the appropriate limit on the spectral power flux density is equal to F_i/β. Values are given in Table I based on $\beta = 25$ MHz or 50 MHz, since for broad-band interference the sensitivity increases with bandwidth.

The sensitivity to interference relative to that for a single antenna with the same values for T_s, β, and λ can be examined by comparing (15) with the equivalent expression for a single antenna, following the analysis in CCIR Report 224-4 [2]. A 12 h averaging time with the single antenna corresponds to $\alpha = 1$ for the array. In the most compact configuration the VLA is less sensitive to interference by 22 dB at 21 cm wavelength and 28 dB at 1.3 cm. In the most extended configuration the equivalent figures are 30 dB and 36 dB, respectively.

TABLE I
HARMFUL INTERFERENCE THRESHOLDS FOR THE VLA DERIVED FROM (15)

		Wavelength Band (cm) 21	6	2	1.3	Units
Continuum observation, narrow-band interference	β	6.25	6.25	6.25	6.25	MHz
	F_i	−166	−152	−140	−135	dB Wm^{-2}
Spectral-line observation, narrow-band interference	β	381	381	381	381	Hz
	F_i	−187	−173	−161	−157	dB Wm^{-2}
Continuum observation, broad-band interference	β	25	50	50	50	MHz
	F_i/β	−237	−225	−213	−208	dB Wm^{-2} Hz^{-1}

VIII. DECORRELATION OF BROAD-BAND INTERFERENCE

Since the signals from cosmic radio sources have the form of broad-band noise, synthesis arrays contain computer-controlled delays to equalize the time delays from the source to the multipliers via each of the antennas. The coherence of the signals is thereby maintained. For broad-band interference that enters the antenna sidelobes, the delays are generally unequal, and the unwanted signal is partially decorrelated. The interference reduction is, in this case, not amenable to a general-case analysis since the delay inequalities are not uniquely defined by the (u, v) coordinates of the antenna pairs. As an example, the effect of interference from a geostationary satellite on the meridian will be examined.

In this analysis it is convenient to measure the relative position of any pair of antennas in terms of the length l of the baseline between them and the hour angle and declination (h, d) of the baseline direction. For radiation from a source with coordinates (H, δ) the difference in the space transmission paths to the two antennas is $l\cos\theta$, where θ is the angle between the direction of the incident radiation and the baseline. This angle is given by

$$\cos\theta = \sin\delta \sin d + \cos\delta \cos d \cos(H - h). \tag{17}$$

For any pair of antennas, lines of constant delay difference on the celestial sphere are small circles concentric with the antenna baseline. As the antennas track, the instrumental delays are adjusted to equalize the paths for the required direction. The circle for which the delays are equalized thus moves across the sky as indicated in Fig. 3. If θ_s is the angle from the baseline for a source being mapped, and θ_i is the angle for a source of interference, the delay inequality t_d for the interfering signal is

$$t_d = l\,|\cos\theta_s - \cos\theta_i|/c, \tag{18}$$

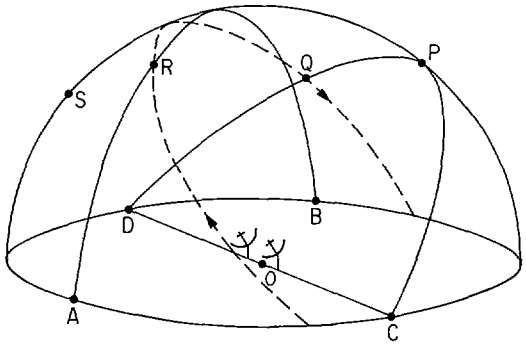

Fig. 3. Celestial hemisphere above observer's horizon and geometrical relationships for one antenna pair. The radio source under observation R moves in a circle centered on the pole P as indicated by the broken line. The angles θ_s and θ_i are DOR and DOS, respectively. The electronic delays are adjusted to equalize path lengths for radiation from all points on curve ARB which is the arc of a circle centered on the antenna baseline direction CD. The arc ARB sweeps across the sky, accompanying the source, and whether or not it ever encompasses the geostationary satellite at S depends upon the observing declination, the baseline direction, and the satellite hour angle. The u component of the antenna spacing goes to zero as the source crosses the point Q on the great circle DQPC which lies in the plane containing the baseline and the pole.

where c is the velocity of light. For a rectangular receiving passband of width β, the response to the interfering signal is reduced by a factor of $\sin(\pi\beta t_d)/\pi\beta t_d$.

The behavior of the decorrelation function, $\sin(\pi\beta t_d)/\pi\beta t_d$, is similar to that of the averaging function (3) except that the latter peaks on the v axis of the (u, v) plane, whereas $\sin(\pi\beta t_d)/\pi\beta t_d$ can peak at any point in the (u, v) plane depending upon the azimuth of the baseline, the position of the interfering source, etc. Those antenna pairs for which the two peaks overlap contribute strongly to the interference in the map, and those for which the peaks are well separated in hour angle contribute relatively little. In making a quantitative estimate of the effect of decorrelation it is therefore necessary to consider the two effects in combination. A factor F_2 can be computed which is the rms of the product of the fringe averaging and decorrelation factors, divided by the rms fringe averaging factor:

$$F_2 = \left[\sum \frac{q' \sin^2(\pi f\tau) \sin^2(\pi\beta t_d)}{(\pi^2 f\tau\beta t_d)^2}\right]^{1/2} \Bigg/ \left[\sum \frac{q' \sin^2(\pi f\tau)}{(\pi f\tau)^2}\right]^{1/2}. \quad (19)$$

F_2 represents the additional interference rejection resulting from decorrelation. The weighting factor q' in (19) is introduced to compensate for the unequal density of points in the (u', v') plane resulting from incremental sampling in hour angle. In the computation, $\delta = -5.5°$ for the geostationary satellite, and for the source H was varied in increments of 30 s from -4 to 4 h. The sums were taken over the hour angle increments and the 351 VLA antenna pairs.

The results are shown as a function of source declination in Fig. 4. The increase in F_2 near the pole results from the decrease in fringe frequency in that region, which causes the peak of $\sin(\pi f\tau)/\pi f\tau$ to broaden and thus overlap the peak in the decorrelation function for a greater number of baselines. The maximum near $-5.5°$ declination occurs because for all antenna pairs the delay inequality for the interference becomes zero as the source passes behind the satellite. As would be expected, F_2 is decreased if the scale of the antenna spacings is increased. One curve is included for a satellite off the meridian, in which an additional maximum appears.

	λ (m)	Δu	B(MHz)	Config.	H_{SAT}
1	0.21	60	25	D	0°
2	0.21	60	25	D	45°
3	0.06	200	50	D	0°
4	0.06	1000	50	A	0°
5	0.013	1000	50	D	0°

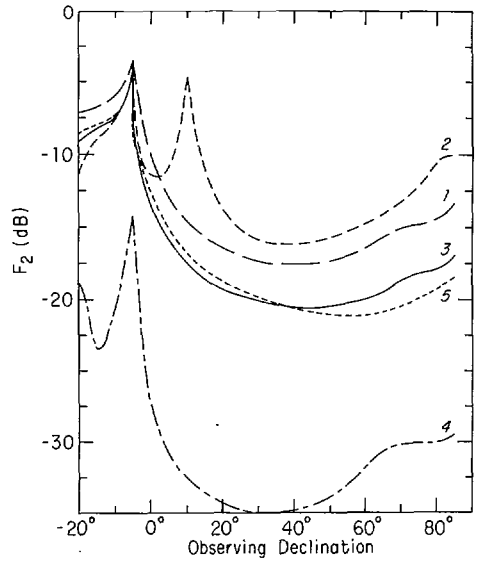

Fig. 4. Curves of F_2, the computed decorrelation factor for broadband interference from a geostationary satellite, as a function of the observing declination for various wavelengths and antenna configurations for the VLA. Configuration D is the most compact and A the most extended. H_{SAT} is the hour angle of the satellite. Values of Δu are in each case about the minimum likely to be used with the other parameters selected.

IX. OTHER EFFECTS

In cases where the mechanisms considered above become very powerful in reducing the response to interference, other effects may determine the harmful thresholds. These have been discussed by Burke [12] for very long baseline interferometry in which the antennas are separated by hundreds or thousands of kilometers, and the possibility of coherent interference being received in two antennas is rather small. Interference in the form of a broad-band noise signal can then limit the sensitivity by increasing the system noise temperature. A similar effect would be expected to result from a narrowband signal which produces the same power level within the receiving passband.

Removal of contaminated visibility data is a possible means of further reducing the response to interference. After averaging in the (u, v) plane, data with unusually high amplitude values located close to the v axis can be deleted. If only a fraction of the v-axis crossings coincide with high sidelobe levels for the interfering signal, the loss of information may be only small, and can largely be compensated by data processing techniques such as the Clean algorithm [13]. It is clearly important to avoid high interference levels in the calibration-source data, and for these such data editing may be particularly useful.

Motion of an interfering transmitter will, on average, increase the frequency of the correlator output variations, and thus enhance the efficiency with which the interference is reduced in averaging over the (u, v) cells. The harmful limits

derived here should therefore be equally applicable to signals from nongeostationary satellites, other than any in very large orbits with apparent angular motion close to that of celestial objects.

X. DISCUSSION

The specification of 0 dBi sidelobe gain for the calculation of harmful thresholds follows the practice in [2] for single-antenna telescopes. If the highest peak sidelobes are omitted, the gain for a large antenna commonly falls to 0 dBi about 19° from the main beam [14]. For many single-antenna telescopes the 0 dBi specification should allow operation to within about 19° of the source of interference. This angular distance is an important consideration since it determines the area of sky lost to the observer. In the present study the sidelobe gain variation is one of the less well-understood aspects. Thus it would be unwise to use the generalized sidelobe model [14] to estimate the angular distance from the main beam at which the levels in Table I become harmful. In situations where this working distance is critical, it may be necessary to adjust the values in Table I by a few decibels in light of future experience.

The use of spaced antennas to discriminate between signals from cosmic and terrestrial sources, or more generally between signals from sources with relative angular motion, offers advantages for purposes other than synthesis mapping. In the search for signals from extraterrestrial intelligence, for example, it will be necessary to search over bands other than those assigned to passive services in order to cover the frequency spectrum adequately. Since obtaining uniform (u, v) coverage is unimportant in this case, conditions that correspond to low values of u can be avoided. The antenna spacing should be chosen so that the natural fringe frequency is high enough to produce a significant interference reduction within the minimum averaging time required in the analysis of the wanted signal. Alternatively, if individual signals can be separated, the occurrance of fringe frequency oscillations can be used to identify those that emanate from sources with nonsidereal motion.

APPENDIX

For cells in the vicinity of the point defined by the radius vector which makes an angle ϕ with the v' axis, the average path length is equal to the cell area, $\Delta u' \Delta v'$, divided by the projected cell width in the q' direction which is $\Delta u(|\sin\phi| + |\csc\delta||\cos\phi|)$. The mean cell-crossing time at position angle ϕ is

$$\tau = \frac{\Delta u\,|\csc\delta|}{q'\omega_0\,(|\sin\phi| + |\csc\delta||\cos\phi|)}. \tag{A1}$$

The mean value of τ^{-1} around a $(u'v')$ locus is

$$\frac{2}{\pi}\int_0^{\pi/2} \tau^{-1}\,d\phi = \frac{2\omega_0 q'}{\pi\Delta u}\,(1 + |\sin\delta|). \tag{A2}$$

ACKNOWLEDGMENT

The author would like to thank Dr. C. B. Moore and Dr. W. P. Winn of the New Mexico Institute of Mining and Technology for permission to use the Langmuir Laboratory on South Baldy for the transmitter location in Section V. Thanks are also due to T. M. Percival and D. L. Grant for valuable assistance in the measurements, and to B. F. Burke, L. R. D'Addario, H. Hvatum, and P. J. Napier for discussions and comments.

REFERENCES

[1] M. Ryle, "A new radio interferometer and its application to the observation of weak radio stars," *Proc. Roy. Soc.*, vol. 211A, pp. 351–375, Mar. 1952.

[2] CCIR, "Characteristics of the radio astronomy service, and interference protection criteria," *Recommendations and Reports*, vol. II, Geneva: Int. Telecommun. Union, Rep. 224–4, pp. 387–400, 1978.

[3] A. R. Thompson, "The effects of the proposed satellite power system on the VLA," in *Workshop on Satellite Power Systems (SPS) Effects on Optical and Radio Astronomy*, P. A. Ekstrom and G. M. Stokes, Eds. U.S. Dept. of Energy, Washington, DC Rep. No. Conf-7905143, pp. 135–142, 1980.

[4] ——, "The effect of a satellite power system on ground-based radio and radar astronomy," *Radio Sci.*, vol. 16, pp. 35–45, 1981.

[5] G. W. Swenson and N. C. Mathur, "The interferometer in radio astronomy," *Proc. IEEE*, vol. 56, pp. 2114–2130, Dec. 1968.

[6] E. B. Fomalont and M. C. H. Wright, "Interferometry and Aperture Synthesis," in *Galactic and Extragalactic Radio Astronomy*, G. L. Verschuur and K. I. Kellermann, Eds. New York: Springer-Verlag, pp. 256–290, 1974.

[7] A. R. Thompson, B. G. Clark, C. M. Wade, and P. J. Napier, "The very large array," *Astrophys J. Suppl.*, vol. 44, pp. 151–167, 1980.

[8] A. R. Thompson and R. N. Bracewell, "Interpolation and Fourier transformation of fringe visibilities," *Astron. J.*, vol. 79, pp. 11–24, Jan. 1974.

[9] A. V. Oppenheim and R. W. Schafer, *Digital Signal Processing*. Englewood Cliffs, NJ: Prentice-Hall, 1975, ch. 3.

[10] CCIR, "Logarithmic quantities and units," *Recommendations and Reports*, vol. XII, Geneva, Int. Telecommun. Union, Recommendation 574, pp. 239–245, 1978.

[11] International Astronomical Union, *Transactions*, vol. 15B, p. 142, 1974.

[12] B. F. Burke, "Satellite power system effects on VLBI," in *Workshop on Satellite Power Systems (SPS) Effects on Optical and Radio Astronomy*, P.A. Ekstrom and G. M. Stokes, Eds. U.S. Dept. of Energy, Washington, D.C. Rep. No. Conf-7905143, pp. 143–145, 1980.

[13] J. A. Högbom, "Aperture synthesis with a non-regular distribution of interferometer baselines," *Astron. Astrophys.* Suppl. 15, pp. 417–426, 1974.

[14] CCIR, "Generalized space research earth station antenna radiation pattern for use in interference calculations, including coordination procedures," *Recommendations and Reports*, vol. II, Geneva: Int. Telecommun. Union, Recommendation 509, pp. 33–34, 1978.

A. Richard Thompson (M'58–SM'81) was born in Hull, Yorkshire, England, on April 7, 1931. He received the B.Sc. degree with honors in physics from the University of Manchester, England. From 1952 to 1956 he was engaged in graduate studies in radio astronomy at Jodrell Bank Experimental Station of the University of Manchester and in 1956 received the Ph.D. degree.

From 1956 to 1957 he worked with E.M.I. Electronics Limited, Feltham, Middlesex, on missile guidance and telemetry problems. He joined the staff of Harvard University, Cambridge, MA, and held the position of Research Associate until 1961 and Research Fellow from 1961 to 1962. During this period he worked in the field of solar radio astronomy at the Fort Davis, Tex., Radio Astronomy Station of Harvard College Observatory. In 1962 he joined Stanford University as a Radio Astronomer and held the position of Senior Research Associate from 1970 to 1972. During this period, from 1966 to 1972, he also held a visiting appointment at the Owens Valley Radio Observatory of the California Institute of Technology. In 1973 he joined the National Radio Astronomy Observatory where he served as Deputy Manager of the VLA program during the initial construction period, and is currently Systems Engineer and Frequency Coordinator for the program.

Dr. Thompson is Chairman of the Radio Astronomy Subcommittee of the Committee on Radio Frequencies of the National Acadamy of Sciences, and subgroup Chairman for Radio Astronomy in U.S. Study Group II of the International Radio Consultative Committee (CCIR). He is a member of U.S. Commission J of the International Union of Radio Science (URSI), Commission 40 of the International Astronomical Union, and the American Astronomical Society.